

The role of the triangle singularity in $\Lambda(1405)$ production in the $\pi^- p \rightarrow K^0 \pi \Sigma$ and $pp \rightarrow p K^+ \pi \Sigma$ processes

M. Bayar,^{1,2,*} R. Pavao,² S. Sakai,² and E. Oset²

¹*Department of Physics, Kocaeli University, 41380 Izmit, Turkey*

²*Departamento de Física Teórica and IFIC, Centro Mixto Universidad de Valencia-CSIC*

Institutos de Investigación de Paterna, Aptdo.22085, 46071 Valencia, Spain

(Dated: July 24, 2018)

We have investigated the cross section for the $\pi^- p \rightarrow K^0 \pi \Sigma$ and $pp \rightarrow p K^+ \pi \Sigma$ reactions paying attention to a mechanism that develops a triangle singularity. The triangle diagram is realized by the decay of a N^* to $K^* \Sigma$ and the K^* decay into πK , and the $\pi \Sigma$ finally merges into $\Lambda(1405)$. The mechanism is expected to produce a peak around 2140 MeV in the $K\Lambda(1405)$ invariant mass. We found that a clear peak appears around 2100 MeV in the $K\Lambda(1405)$ invariant mass which is about 40 MeV lower than the expectation, and that is due to the resonance peak of a N^* resonance which plays a crucial role in the $K^* \Sigma$ production. The mechanism studied produces the peak of the $\Lambda(1405)$ around or below 1400 MeV, as is seen in the $pp \rightarrow p K^+ \pi \Sigma$ HADES experiment.

PACS numbers:

I. INTRODUCTION

The nature of the $\Lambda(1405)$, the lowest excitation of Λ with $J^P = 1/2^-$, has been given much attention for a long time. The quark model predicts the mass at higher energy than the observed peak [1], and a description of the $\Lambda(1405)$ as a $\bar{K}N$ molecular state shows a good agreement with the experimental result, as originally pointed out in Refs. [2–4]. The studies of the $\bar{K}N$ system based on SU(3) chiral symmetry with the implementation of unitarity and coupled channels suggest that the $\Lambda(1405)$ is generated as a $\bar{K}N$ quasi-bound state [5–16]. The recent analysis of the lattice QCD simulation supports the molecular picture of the $\Lambda(1405)$ [17, 18]. Furthermore, the analysis of the compositeness [19–21] which is a measure of the hadronic molecular component, the charge radius [22], and the root mean square radius [23], also support the picture of the $\Lambda(1405)$ as a $\bar{K}N$ molecule. Other than these works, many studies for the $\Lambda(1405)$ production from the photon-induced reaction [24–29], the pion-induced one [30, 31], the kaon-induced one [32–35], the proton-proton collision [36, 37], and the heavy meson decay [38] were carried out to clarify the nature of the $\Lambda(1405)$ resonance. The studies related to the $\bar{K}N$ system are summarized in Refs. [39, 40] (see also note in the PDG [41]).

In Ref. [29], the role of the triangle singularity (TS) on the angle and the energy dependence of the $\Lambda(1405)$ photoproduction was studied. The triangle singularity was first pointed out in Ref. [42]. The correspond-

ing Feynman diagram is formed by a sequential decay of a hadron and a fusion of two of them, and the amplitude associated with the diagram has a singularity if the process has a classical counterpart, which is known as Coleman-Norton theorem [43]. The studies of many processes including the triangle singularity elucidate the possible effect of the triangle singularity on the hadron properties, *e.g.*, the $\eta(1405)$ decay into $\pi^0 a_0$ or $\pi^0 f_0$ [44–46], the possible origin of $Z_c(3900)$ [47–49], the speculation on the pentaquark candidate P_c [50–52] (see Ref. [53] for a critical discussion to the light of the preferred experimental quantum numbers [54]), the B_s decay into $B\pi\pi$ [55] and B^- decays [56, 57]. Here, we note that the strength of the triangle peak is tightly connected with the coupling strength of the two hadrons merging into a third one. For example, in the study of the B^- decay into $K^-\pi^- D_{s0}^+(D_{s1}^+)$ [56], the DK (D^*K) in the triangle loop goes into D_{s0} (D_{s1}), which is dynamically generated from the DK (D^*K) and has a large coupling to this channel [58, 59]. Then, the observation of the peak from the triangle mechanism would give an additional support for the hadronic molecular picture of these states.

For further understanding of the nature of the $\Lambda(1405)$ and triangle mechanisms, in this paper we investigate the $\pi^- p \rightarrow K^0 \pi \Sigma$ and $pp \rightarrow p K^+ \pi \Sigma$ processes including a triangle diagram. In both processes, the triangle diagram is formed by a N^* decay into $K^* \Sigma$ followed by the decay of K^* into πK and the fusion of the $\pi \Sigma$ to form the $\Lambda(1405)$, which finally decays into $\pi \Sigma$. In this process, the $K^* \pi \Sigma$ loop generates a triangle singularity around 2140 MeV in the invariant mass of $K\Lambda(1405)$ from the formula given by Eq. (18) of Ref. [53]. The corresponding diagram is shown in Fig. 1. The N^* resonance which strongly couples to $K^* \Sigma$ is obtained in Ref. [60] based on the hidden lo-

*Electronic address: melahat.bayar@kocaeli.edu.tr

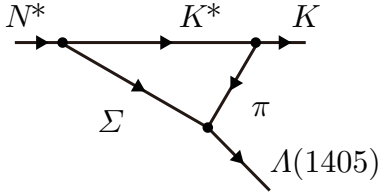


FIG. 1: Triangle diagram for the $\Lambda(1405)$ production from a N^* resonance.

cal symmetry and the chiral unitary approach, and the analysis of the $K\Sigma$ photoproduction off nucleon around the $K^*\Lambda$ threshold energy suggests that the resonance is responsible for the observed cross section [61].

As the result of our calculation, we found a peak in the $K\Lambda(1405)$ mass distribution around 2100 MeV in both reactions, which is lowered with respect to the 2140 MeV given by the TS master formula [53] by the initial N^* resonance which peaks around 2030 MeV. The experimental study on the $\Lambda(1405)$ production from the π^-p is reported in Refs. [62, 63], but the energy is too small for the triangle singularity from the $K^*\pi\Sigma$ loop to be observed. The production of the $\Lambda(1405)$ from the proton-proton collision is studied in Refs. [64–66]. The future observation of the inevitable peak from the triangle mechanism induced by the $\Lambda(1405)$ would give further support for the molecular nature of the $\Lambda(1405)$.

II. FORMALISM

A. $\pi^-p \rightarrow K^0\pi^+\Sigma^-$

In this subsection we will study the effects of the triangle loop in the following decays: $\pi^-p \rightarrow K^0\pi^+\Sigma^-$, $\pi^-p \rightarrow K^0\pi^0\Sigma^0$ and $\pi^-p \rightarrow K^0\pi^-\Sigma^+$. The diagrams where the triangle singularity can appear for those reactions are shown in Fig. 2. To evaluate the differential cross section associated with this diagram we will use

$$\frac{d\sigma_{K^0\pi\Sigma}}{dm_{\text{inv}}} = \frac{M_p M_\Sigma}{2(2\pi)^3 s} \frac{|\vec{k}| |\vec{p}_\pi|}{|\vec{p}_\pi|} \sum \sum |t_{\pi^-p \rightarrow K^0\pi\Sigma}|^2, \quad (\text{II.1})$$

with m_{inv} the invariant mass of the final $\pi\Sigma$,

$$|\vec{p}_\pi| = \frac{\lambda^{\frac{1}{2}}(s, m_\pi^2, M_N^2)}{2\sqrt{s}}, \quad (\text{II.2})$$

the momentum of the initial π^- in the π^-p center-of-mass frame (CM),

$$|\vec{k}| = \frac{\lambda^{\frac{1}{2}}(s, m_K^2, m_{\text{inv}}^2)}{2\sqrt{s}}, \quad (\text{II.3})$$

the momentum of the final K^0 in the π^-p CM, and

$$|\vec{p}_\pi| = \frac{\lambda^{\frac{1}{2}}(m_{\text{inv}}^2, m_\pi^2, M_\Sigma^2)}{2m_{\text{inv}}}, \quad (\text{II.4})$$

the momentum of the final π in the $\pi\Sigma$ CM.

The resonance $N^*(2030)$ could have $J^P = \frac{1}{2}^-$ or $J^P = \frac{3}{2}^-$ as stated in Refs. [60, 61] with a width $\Gamma_{N^*} \simeq 125$ MeV, but in order to have $J = 3/2$ in π^-p we need p -wave and then we have positive parity. Hence, we take π^-p in $L = 0$ and hence $J_{N^*}^P = \frac{1}{2}^-$. In the isospin basis the $\pi^-p \rightarrow N^*$ vertex has then the form

$$-it_{\pi^-p, N^*} = -ig_{\pi^-p, N^*}^{I=\frac{1}{2}}. \quad (\text{II.5})$$

To estimate the $g_{\pi^-p, N^*}^{I=\frac{1}{2}}$ we assume that $\Gamma_{N^*, \pi N}$ is of the order of 70 MeV and then use the formula,

$$\Gamma_{N^*, \pi N} = \frac{1}{2\pi} \frac{M_\Sigma}{M_{N^*}} (g_{\pi^-p, N^*}^{I=\frac{1}{2}})^2 |\vec{p}_\pi| \quad (\text{II.6})$$

with M_{N^*} the mass of $N^*(2030)$. Here, $|\vec{p}_\pi|$ is the momentum of π that results from the decay of N^* and is evaluated using Eq. (II.2), $s = M_{N^*}^2$. Finally, we obtain $g_{\pi^-p, N^*}^{I=\frac{1}{2}} \simeq 1.1$.

Since we will have different amplitudes if we change the charge of the intermediate $\pi\Sigma$ particles, it is convenient to go from the isospin basis ($|I, I_3\rangle$) to the charge basis. Using the Clebsch-Gordan coefficients, we have

$$|\pi^-p\rangle = \sqrt{\frac{1}{3}} \left| \frac{3}{2}, -\frac{1}{2} \right\rangle - \sqrt{\frac{2}{3}} \left| \frac{1}{2}, -\frac{1}{2} \right\rangle. \quad (\text{II.7})$$

This means that the coupling of π^-p to N^* will be

$$g_{\pi^-p, N^*} = -\sqrt{\frac{2}{3}} g_{\pi^-p, N^*}^{I=\frac{1}{2}} \quad (\text{II.8})$$

The $N^*(2030) \rightarrow K^*\Sigma$ process occurs in s -wave, then the amplitude is written as

$$-it_{N^*, K^*\Sigma} = -ig_{N^*, K^*\Sigma} \vec{\sigma} \cdot \vec{\epsilon}_{K^*}. \quad (\text{II.9})$$

From Ref. [60], we get $g_{N^*, K^*\Sigma}^{I=\frac{1}{2}} = 3.9 + i0.2$, and since we have both Σ^-K^{*+} and Σ^0K^{*0} (Figs. 2a and 2b respectively), then, using

$$|\Sigma^0 K^{*0}\rangle = \sqrt{\frac{2}{3}} \left| \frac{3}{2}, -\frac{1}{2} \right\rangle + \sqrt{\frac{1}{3}} \left| \frac{1}{2}, -\frac{1}{2} \right\rangle, \quad (\text{II.10a})$$

$$|\Sigma^- K^{*+}\rangle = \sqrt{\frac{1}{3}} \left| \frac{3}{2}, -\frac{1}{2} \right\rangle - \sqrt{\frac{2}{3}} \left| \frac{1}{2}, -\frac{1}{2} \right\rangle, \quad (\text{II.10b})$$

we get

$$g_{N^*, \Sigma^0 K^{*0}} = \sqrt{\frac{1}{3}} g_{N^*, \Sigma K^*}^{I=\frac{1}{2}}, \quad (\text{II.11a})$$

$$g_{N^*, \Sigma^- K^{*+}} = -\sqrt{\frac{2}{3}} g_{N^*, \Sigma K^*}^{I=\frac{1}{2}}. \quad (\text{II.11b})$$

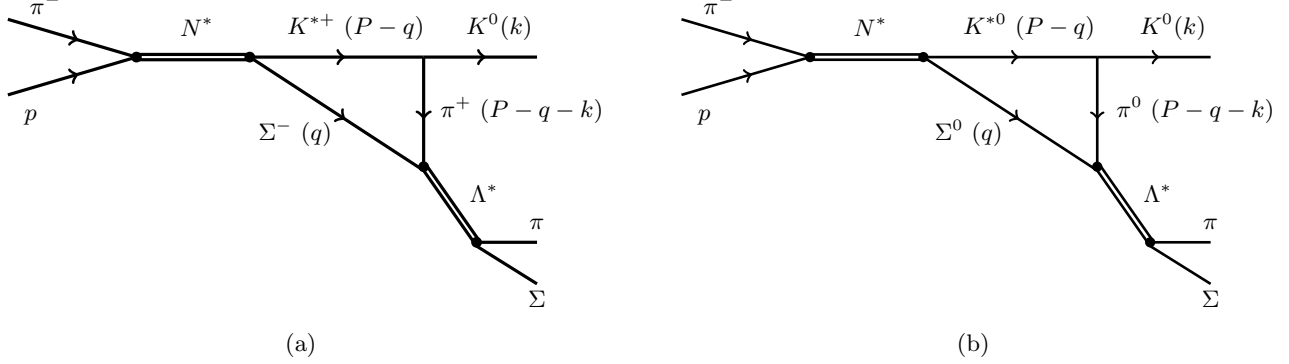


FIG. 2: Diagrams for the reaction $\pi^- p \rightarrow K^0 \pi \Sigma$ that contain the triangle mechanism, where $\pi \Sigma$ can be $\pi^- \Sigma^+$, $\pi^0 \Sigma^0$ and $\pi^+ \Sigma^-$.

Then, for the amplitude of the $\pi^- p \rightarrow \Sigma K^*$ reaction through $N^*(2030)$, we have

$$t_{\pi^- p, \Sigma^0 K^{*0}} = \frac{g_{\pi^- p, N^*} g_{N^*, \Sigma^0 K^{*0}}}{\sqrt{s} - M_{N^*} + i\frac{\Gamma_{N^*}}{2}} \vec{\sigma} \cdot \vec{\epsilon}_{K^*}, \quad (\text{II.12a})$$

$$t_{\pi^- p, \Sigma^- K^{*+}} = \frac{g_{\pi^- p, N^*} g_{N^*, \Sigma^- K^{*+}}}{\sqrt{s} - M_{N^*} + i\frac{\Gamma_{N^*}}{2}} \vec{\sigma} \cdot \vec{\epsilon}_{K^*}. \quad (\text{II.12b})$$

Now, the $K^{*+} \rightarrow K^0 \pi^+$ vertex can be calculated using the chiral invariant Lagrangian with local hidden symmetry given in Refs. [67–70],

$$\mathcal{L}_{VPP} = -ig \langle [\Phi, \partial_\mu \Phi] V^\mu \rangle. \quad (\text{II.13})$$

The symbol $\langle \dots \rangle$ here represents the trace over the SU(3) flavor matrices, and the coupling is $g = m_V/2f_\pi$, with $m_V = 800$ MeV and $f_\pi = 93$ MeV. The SU(3) matrices for the pseudoscalar and vector octet mesons Φ and V^μ are given by

$$\Phi = \begin{pmatrix} \frac{1}{\sqrt{2}}\pi^0 + \frac{1}{\sqrt{6}}\eta & \pi^+ & K^+ \\ \pi^- & -\frac{1}{\sqrt{2}}\pi^0 + \frac{1}{\sqrt{6}}\eta & K^0 \\ K^- & \bar{K}^0 & -\sqrt{\frac{2}{3}}\eta \end{pmatrix}, \quad (\text{II.14})$$

$$V_\mu = \begin{pmatrix} \frac{1}{\sqrt{2}}\rho_\mu^0 + \frac{1}{\sqrt{2}}\omega_\mu & \rho_\mu^+ & K_\mu^{*+} \\ \rho_\mu^- & -\frac{1}{\sqrt{2}}\rho_\mu^0 + \frac{1}{\sqrt{2}}\omega_\mu & K_\mu^{*0} \\ K_\mu^{*-} & \bar{K}_\mu^{*0} & \phi_\mu \end{pmatrix}. \quad (\text{II.15})$$

From Eq. (II.13) we get

$$-it_{K^{*+}, K^0 \pi^+} = -ig \epsilon_{K^*}^\mu (p_{K^0} - p_{\pi^+})_\mu \quad (\text{II.16})$$

$$= ig \epsilon_{K^*}^\mu (P - q - 2k)_\mu \quad (\text{II.17})$$

$$\simeq ig \vec{\epsilon}_{K^*} \cdot (\vec{q} + 2\vec{k}), \quad (\text{II.18})$$

where in the last step we made a nonrelativistic approximation, neglecting the $\epsilon_{K^*}^0$ component. This is

very accurate when the momentum of the K^* is small compared to its mass. We shall evaluate the triangle diagram in the ΣK^* CM, where the on-shell momentum of the K^* is about 250 MeV/c at $M_{\text{inv}}(\Sigma K^*) \simeq 2140$ MeV where the triangle singularity appears. In Ref. [56] it is shown that the effect of neglecting the ϵ^0 component goes as $(p_{K^*}/m_{K^*})^2$, with a coefficient in front that renders this correction negligible.

Similarly, for $K^{*0} \rightarrow K^0 \pi^0$ we get

$$-it_{K^{*0}, K^0 \pi^0} = -i \frac{1}{\sqrt{2}} g \vec{\epsilon}_{K^*} \cdot (\vec{q} + 2\vec{k}). \quad (\text{II.19})$$

The final vertex that we need to calculate in the diagrams of Fig.1 is $t_{\Sigma \pi, \Sigma \pi}$ which is given by the $\Sigma \pi \rightarrow \Lambda(1405) \rightarrow \Sigma \pi$ amplitude studied in Ref. [6] based on chiral unitary approach. There, the authors use the lowest order meson-baryon chiral lagrangian

$$\mathcal{L}_1^{(B)} = \left\langle \bar{B} i \gamma^\mu \frac{1}{4f^2} [(\Phi \partial_\mu \Phi - \partial_\mu \Phi \Phi) B - B (\Phi \partial_\mu \Phi - \partial_\mu \Phi \Phi)] \right\rangle, \quad (\text{II.20})$$

with,

$$B = \begin{pmatrix} \frac{1}{\sqrt{2}}\Sigma^0 + \frac{1}{\sqrt{6}}\Lambda & \Sigma^+ & p \\ \Sigma^- & -\frac{1}{\sqrt{2}}\Sigma^0 + \frac{1}{\sqrt{6}}\Lambda & n \\ \Xi^- & \Xi^0 & -\sqrt{\frac{2}{3}}\Lambda \end{pmatrix}. \quad (\text{II.21})$$

The Bethe-Salpeter equation is then used to calculate the meson-baryon amplitude,

$$t = [1 - VG]^{-1} V, \quad (\text{II.22})$$

where t , V , and G are the meson-baryon amplitude, interaction kernel, and meson-baryon loop function, respectively. For the evaluation of t , we use the momentum cutoff $q_{\text{max}} = 630$ MeV for the loop function G , and $f = 1.15f_\pi$ with the pion decay constant $f_\pi = 93$ MeV as done in Ref. [6].

Thus, the amplitude associated with the diagram in

Fig. 2a, that we call t_1 , is given by

$$t_1 = -i \frac{2}{3} \frac{g_{\pi N, N^*}^{I=\frac{1}{2}} g_{N^*, \Sigma K^*}^{I=\frac{1}{2}}}{\sqrt{s} - M_{N^*} + i \frac{\Gamma_{N^*}}{2}} g \sum_{\text{pol. of } K^*} \int \frac{d^4 q}{(2\pi)^4} \frac{2M_\Sigma \vec{\sigma} \cdot \vec{\epsilon}_{K^*}}{q^2 - M_\Sigma^2 + i\epsilon} \frac{(2\vec{k} + \vec{q}) \cdot \vec{\epsilon}_{K^*}}{(P - q)^2 - m_{K^*}^2 + i\epsilon} \frac{t_{\Sigma^- \pi^+, \Sigma \pi}}{(P - q - k)^2 - m_\pi^2 + i\epsilon}. \quad (\text{II.23})$$

Using the following property,

$$\int d^3 q q_i f(\vec{q}, \vec{k}) = k_i \int d^3 q \frac{\vec{q} \cdot \vec{k}}{|\vec{k}|^2} f(\vec{q}, \vec{k})$$

with $f(\vec{q}, \vec{k})$ the three propagators in the integrand of Eq. (II.23), and the formula in the nonrelativistic approximation,

$$\sum_{\text{pol.}} \epsilon_{K^*i} \epsilon_{K^*j} = \delta_{ij},$$

Eq. (II.23) becomes

$$t_1 = -\frac{4M_\Sigma}{3} \frac{g_{\pi N, N^*}^{I=\frac{1}{2}} g_{N^*, \Sigma K^*}^{I=\frac{1}{2}}}{\sqrt{s} - M_{N^*} + i \frac{\Gamma_{N^*}}{2}} g \vec{\sigma} \cdot \vec{k} t_T t_{\Sigma^- \pi^+, \Sigma \pi}, \quad (\text{II.24})$$

with

$$t_T = i \int \frac{d^4 q}{(2\pi)^4} \left(2 + \frac{\vec{q} \cdot \vec{k}}{|\vec{k}|^2} \right) \frac{1}{q^2 - M_\Sigma^2 + i\epsilon} \frac{1}{(P - q)^2 - m_{K^*}^2 + i\epsilon} \frac{1}{(P - q - k)^2 - m_\pi^2 + i\epsilon}. \quad (\text{II.25})$$

Integrating t_T over q^0 , we get [53, 71],

$$t_T = \int \frac{d^3 q}{(2\pi)^3} \left(2 + \frac{\vec{q} \cdot \vec{k}}{|\vec{k}|^2} \right) \frac{1}{8\omega^* \omega \omega'} \frac{1}{k^0 - \omega' - \omega^*} \frac{1}{P^0 + \omega + \omega' - k^0} \frac{1}{P^0 - \omega - \omega' - k^0 + i\epsilon} \times \frac{\{2P^0 \omega + 2k^0 \omega' - 2[\omega + \omega'][\omega + \omega' + \omega^*]\}}{P^0 - \omega^* - \omega + i\epsilon}, \quad (\text{II.26})$$

where $P^0 = \sqrt{s}$, $\omega^*(\vec{q}) = \sqrt{m_{K^{*0}}^2 + |\vec{q}|^2}$, $\omega'(\vec{q}) = \sqrt{m_\pi^2 + |\vec{q} + \vec{k}|^2}$ and $\omega(\vec{q}) = \sqrt{M_\Sigma^2 + |\vec{q}|^2}$. We regularize the integral in Eq. (II.26) by using the same cutoff of the meson loop in Eq. (II.22), $\theta(q_{\max} - |\vec{q}^*|)$, where \vec{q}^* is the Σ momentum in the final $\pi \Sigma$ CM [53] and $q_{\max} = 630$ MeV. The width of K^* is taken into account by replacing ω^* with $\omega^* - i \frac{\Gamma_{K^*}}{2}$.

For the case when $N^*(2030) \rightarrow K^{*+} \Sigma^-$, t_2 , we have

$$t_2 = -\frac{2M_\Sigma}{3} \frac{g_{\pi N, N^*}^{I=\frac{1}{2}} g_{N^*, \Sigma K^*}^{I=\frac{1}{2}}}{\sqrt{s} - M_{N^*} + i \frac{\Gamma_{N^*}}{2}} g \vec{\sigma} \cdot \vec{k} t_T t_{\Sigma^0 \pi^0, \Sigma \pi}. \quad (\text{II.27})$$

Thus, the total amplitude in Eq. (II.1) associated with $\pi^- p \rightarrow K^0 \pi \Sigma$ becomes

$$t_{\pi^- p \rightarrow K^0 \pi \Sigma} = t_1 + t_2 = C \vec{\sigma} \cdot \vec{k} t_T (t_{\Sigma^- \pi^+, \Sigma \pi} + \frac{1}{2} t_{\Sigma^0 \pi^0, \Sigma \pi}), \quad (\text{II.28})$$

with

$$C = -\frac{2}{3} g_{\pi N, N^*}^{I=\frac{1}{2}} g_{N^*, \Sigma K^*}^{I=\frac{1}{2}} g \frac{2M_\Sigma}{\sqrt{s} - M_{N^*} + i\frac{\Gamma_{N^*}}{2}}. \quad (\text{II.29})$$

Here, the t_T associated with the diagrams in Figs. 2a

and 2b are the same because we use the isospin averaged mass and width of the hadrons in t_T .

Calculating the square of the amplitude and summing and averaging over the spins we get

$$\sum \sum |t_{\pi^- p \rightarrow K^0 \pi \Sigma}|^2 = |C|^2 |\vec{k}|^2 |t_T|^2 |t_{\Sigma^- \pi^+, \Sigma \pi} + \frac{1}{2} t_{\Sigma^0 \pi^0, \Sigma \pi}|^2 \quad (\text{II.30})$$

Finally, using Eq. (II.30) in Eq. (II.1) we can calculate the $\frac{d\sigma_{K^0 \pi \Sigma}}{dm_{\text{inv}}}$ associated with the diagrams in Fig. 2.

B. $pp \rightarrow p K^+ \pi \Sigma$

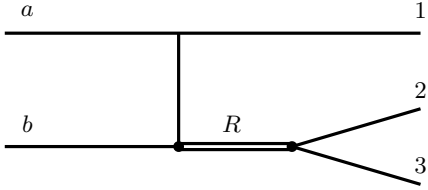


FIG. 3: Diagram of $a b \rightarrow 1 R \rightarrow 1 2 3$.

Now we will study the effects of the triangle loop in the following decays: $pp \rightarrow p K^+ \pi^+ \Sigma^-$, $pp \rightarrow p K^+ \pi^0 \Sigma^0$ and $pp \rightarrow p K^+ \pi^- \Sigma^+$. For this, we will first start analysing the diagram in Fig. 3. For this diagram, the differential cross section is calculated using the formula in Ref. [72],

$$\frac{d^2\sigma}{dt dM_{\text{inv}}} = \frac{\Pi_F(2M_F)}{32p_a^2 s (2\pi)^3} |\vec{p}_2| \sum \sum |t_{ab \rightarrow 123}|^2, \quad (\text{II.31})$$

with $t = (p_a - p_1)^2$, M_{inv} the invariant mass of particles 2 and 3, \vec{p}_2 the momentum of particle 2 in the 23 CM, such that

$$|\vec{p}_2| = \frac{\lambda^{\frac{1}{2}}(M_{\text{inv}}^2, m_2^2, m_3^2)}{2M_{\text{inv}}}, \quad (\text{II.32})$$

p_a the momentum of the particle a in the initial state,

$$p_a = \frac{\lambda^{\frac{1}{2}}(s, M_a^2, M_b^2)}{2\sqrt{s}}, \quad (\text{II.33})$$

and $\Pi_F(2M_F)$ means that we multiply $2M_F$ for each fermion in Fig. 3, where M_F is the mass of the respective fermion. This factor appears because we use the normalization of Ref. [73].

The complete diagrams for our reaction are shown in Fig. 4. The triangle part of the diagrams is very similar to the last case, except that because of charge conservation the particles in the loop will be different. Thus, instead of Eqs. (II.10a) and (II.10b), we will have

$$|\Sigma^+ K^{*0}\rangle = -\sqrt{\frac{1}{3}} \left| \frac{3}{2}, \frac{1}{2} \right\rangle - \sqrt{\frac{2}{3}} \left| \frac{1}{2}, \frac{1}{2} \right\rangle, \quad (\text{II.34a})$$

$$|\Sigma^0 K^{*+}\rangle = \sqrt{\frac{2}{3}} \left| \frac{3}{2}, \frac{1}{2} \right\rangle - \sqrt{\frac{1}{3}} \left| \frac{1}{2}, \frac{1}{2} \right\rangle, \quad (\text{II.34b})$$

where, to match the sign convention of the Φ and B matrices, we used $|\Sigma^+\rangle = -|1 1\rangle$ (see Ref. [74] for further discussion). Then, we get $g_{N^*, \Sigma^+ K^{*0}} = -\sqrt{2/3} g_{N^*, \Sigma K^*}^{I=\frac{1}{2}}$ and $g_{N^*, \Sigma^0 K^{*+}} = -\sqrt{1/3} g_{N^*, \Sigma K^*}^{I=\frac{1}{2}}$.

The vertices $K^{*0} \rightarrow K^+ \pi^-$ and $K^{*+} \rightarrow K^+ \pi^0$ are calculated using Eq. (II.13), which gives

$$-it_{K^{*0}, K^+ \pi^-} = ig(\vec{q} + 2\vec{k}) \cdot \vec{\epsilon}_{K^*}, \quad (\text{II.35a})$$

$$-it_{K^{*+}, K^+ \pi^0} = i\frac{g}{\sqrt{2}}(\vec{q} + 2\vec{k}) \cdot \vec{\epsilon}_{K^*} \quad (\text{II.35b})$$

To calculate the cross section for the diagrams in Fig. 4, we proceed as done in Ref. [72]. In Fig. 3, the t matrix found in Eq. (II.31) is given by

$$t_{ab \rightarrow 123} = C' \frac{1}{M_{\text{inv}} - M_R + i\frac{\Gamma_R}{2}} g_{R,23}, \quad (\text{II.36})$$

with C' a parameter that carries the dependence of the amplitude on the variable t as well as information about the $pp \rightarrow pR$ transition. Substituting

$$\Gamma_{R,23} = \frac{1}{2\pi} \frac{M_3}{M_{\text{inv}}} g_{R,23}^2 |\vec{p}_2|, \quad (\text{II.37})$$

where particle 3 is assumed to be a baryon, into Eq. (II.31), we get

$$\frac{d^2\sigma}{dt dM_{\text{inv}}} = \frac{\prod_F (2M_F)}{32p_a^2 s(2\pi)^3} |C'|^2 \left| \frac{1}{M_{\text{inv}} - M_R + i\frac{\Gamma_R}{2}} \right|^2 2\pi \frac{M_{\text{inv}}}{M_3} \Gamma_{R,23}. \quad (\text{II.38})$$

Now we can take into account the complete reaction by substituting $\Gamma_{R,23}$ for $\Gamma_{N^* \rightarrow K^+ \pi\Sigma}$, where

$$\frac{d\Gamma_{N^* \rightarrow K^+ \pi\Sigma}}{dm_{\text{inv}}} = \frac{2M_{N^*} 2M_\Sigma}{(2\pi)^3 4M_{\text{inv}}^2} |\vec{p}_K| |\vec{p}_\pi| \overline{\sum} \sum |t'|^2, \quad (\text{II.39})$$

with $|\vec{p}_K|$ the momentum of K in the rest frame of N^* ,

$$|\vec{p}_K| = \frac{\lambda^{\frac{1}{2}}(M_{\text{inv}}^2, m_K^2, m_{\text{inv}}^2)}{2M_{\text{inv}}}, \quad (\text{II.40})$$

and $|\vec{p}_\pi|$ the π momentum in the $\pi\Sigma$ CM given by Eq. (II.4).

Then, from Eq. (II.38) we obtain

$$\frac{d^3\sigma_{pK^+ \pi\Sigma}}{dt dM_{\text{inv}} dm_{\text{inv}}} = \frac{(2M_p)^3 2M_\Sigma}{32p_a^2 s(2\pi)^5} |\vec{p}_K| |\vec{p}_\pi| |C'|^2 \left| \frac{1}{M_{\text{inv}} - M_{N^*} + i\frac{\Gamma_{N^*}}{2}} \right|^2 \overline{\sum} \sum |t'|^2. \quad (\text{II.41})$$

The transition amplitude t' in Eq. (II.41) is

$$t' = \sqrt{\frac{2}{3}} 2M_\Sigma g_{N^*, \Sigma K^*}^{I=\frac{1}{2}} g(t_{\Sigma^+ \pi^-, \Sigma \pi} + \frac{1}{2} t_{\Sigma^0 \pi^0, \Sigma \pi}) \vec{\sigma} \cdot \vec{k} t_T, \quad (\text{II.42})$$

which is constructed in a similar way to what was done in the previous subsection to obtain Eq. (II.28) but now changing the following variables in Eq. (II.26),

$$P^0 = M_{\text{inv}} \quad (\text{II.43a})$$

$$|\vec{k}| = |\vec{p}_K| = \frac{\lambda^{\frac{1}{2}}(M_{\text{inv}}^2, m_K^2, m_{\text{inv}}^2)}{2M_{\text{inv}}} \quad (\text{II.43b})$$

$$k^0 = \frac{M_{\text{inv}}^2 + m_K^2 - m_{\text{inv}}^2}{2M_{\text{inv}}} \quad (\text{II.43c})$$

Putting Eq. (II.42) into Eq. (II.41) we get

$$\frac{d^3\sigma_{pK^+ \pi\Sigma}}{dt dM_{\text{inv}} dm_{\text{inv}}} = C'' \frac{1}{|M_{\text{inv}} - M_{N^*} + i\frac{\Gamma_{N^*}}{2}|^2} |\vec{p}_\pi| |t_{\Sigma^+ \pi^-, \Sigma \pi} + \frac{1}{2} t_{\Sigma^0 \pi^0, \Sigma \pi}|^2 |\vec{k}|^3 |t_T|^2, \quad (\text{II.44})$$

where $|\vec{p}_\pi|$ is the π momentum in the $\pi\Sigma$ CM,

and

$$|\vec{p}_\pi| = \frac{\lambda^{\frac{1}{2}}(m_{\text{inv}}^2, m_\pi^2, M_\Sigma^2)}{2m_{\text{inv}}}, \quad (\text{II.45})$$

$$C'' = \frac{2}{3} \frac{(2M_p)^3 2M_\Sigma}{32p_a^2 s(2\pi)^5} |g_{N^*, \Sigma K^*}^{I=\frac{1}{2}}|^2 g^2 (2M_\Sigma)^2 |C'|^2, \quad (\text{II.46})$$

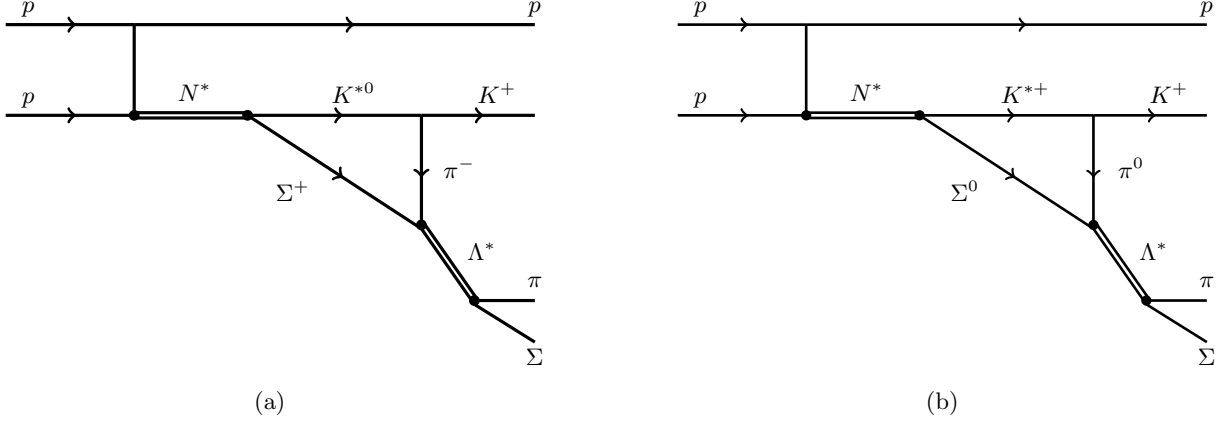


FIG. 4: Diagrams for the reaction $pp \rightarrow pK^+\pi\Sigma$ that contain the triangle mechanism, where $\pi\Sigma$ can be $\pi^-\Sigma^+$, $\pi^0\Sigma^0$ and $\pi^+\Sigma^-$.

which is a function of $s = (p_a + p_b)^2$ and $t = (p_a - p_1)^2$.

Using now the relation

$$dt = 2|\vec{p}_a||\vec{p}_1| d\cos\theta, \quad (\text{II.47})$$

which follows from $t = (p_a - p_1)^2$, then we obtain

$$\frac{d^3\sigma_{pK^+\pi\Sigma}}{d\cos\theta dM_{\text{inv}} dm_{\text{inv}}} = C'' \frac{2|\vec{p}_a||\vec{p}_1|}{|M_{\text{inv}} - M_{N^*} + i\frac{\Gamma_{N^*}}{2}|^2} |\vec{p}_\pi| |t_{\Sigma^+\pi^-, \Sigma\pi} + \frac{1}{2} t_{\Sigma^0\pi^0, \Sigma\pi}|^2 |\vec{k}|^3 |t_T|^2, \quad (\text{II.48})$$

with

$$|\vec{p}_a| = \frac{\lambda^{\frac{1}{2}}(s, M_p^2, M_p^2)}{2\sqrt{s}}, \quad (\text{II.49a})$$

$$|\vec{p}_1| = \frac{\lambda^{\frac{1}{2}}(s, M_p^2, M_{\text{inv}}^2)}{2\sqrt{s}}. \quad (\text{II.49b})$$

This last step is important to account for the phase space of this process that depends on $|\vec{p}_1|$, which is tied

to M_{inv} .

Finally, we should integrate out the $\cos\theta$ in Eq. (II.48) but C' in C'' depend on it. The resultant factor of the $\cos\theta$ integration is denoted by C''' and since we do not know the expression for C' , we take $C''' = 1$. This means that from now on we will use arbitrary units (a.u.) for the cross section.

Thus, we end up with

$$\frac{d^2\sigma_{pK^+\pi\Sigma}}{dM_{\text{inv}} dm_{\text{inv}}} = \frac{C''' 2|\vec{p}_a||\vec{p}_1|}{|M_{\text{inv}} - M_{N^*} + i\frac{\Gamma_{N^*}}{2}|^2} |\vec{p}_\pi| |t_{\Sigma^+\pi^-, \Sigma\pi} + \frac{1}{2} t_{\Sigma^0\pi^0, \Sigma\pi}|^2 |\vec{k}|^3 |t_T|^2. \quad (\text{II.50})$$

III. RESULTS

In Fig. 5, we show the real, imaginary part and absolute value of the amplitude t_T of Eq. (II.26) as a function of the invariant mass of the $K\Lambda(1405)$, M_{inv} ,

by fixing the invariant mass of $\pi\Sigma$, m_{inv} , at 1400 MeV. The absolute value of t_T has a peak around 2140 MeV as expected from the condition for a triangular singularity by Eq. (18) of Ref. [53], and the peak is dominated by the imaginary part of the amplitude. As mentioned in

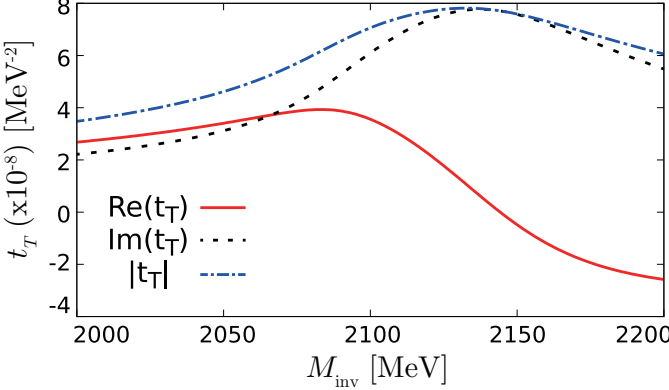


FIG. 5: $\text{Re}(t_T)$, $\text{Im}(t_T)$ and $|t_T|$ of Eq. (II.26).

Ref. [56], the peak of the imaginary part is responsible for the triangle singularity.

In Fig. 6, we plot the mass distribution of the $\pi^- p \rightarrow K^0 \pi\Sigma$ scattering process as a function of $m_{\text{inv}}(\pi^0 \Sigma^0)$, $m_{\text{inv}}(\pi^+ \Sigma^-)$ and $m_{\text{inv}}(\pi^- \Sigma^+)$ with a fixed of $\sqrt{s} = M_{\text{inv}} = 2050, 2100, 2140, 2200, 2230$ MeV. Let us first look at the $\pi^0 \Sigma^0$ mass distribution in Fig. 6. At $M_{\text{inv}} = 2140$ MeV, where a peak associated with the triangle singularity is expected from the formula in Ref. [53], we can see a clear peak at 1400 MeV associated with $\Lambda(1405)$ in the $\pi\Sigma$ invariant mass. As we see in the figure the largest strength is obtained with $M_{\text{inv}} = 2100$ MeV. A peak is found around 1385 MeV for $M_{\text{inv}} = 2200, 2230$ MeV with a smaller strength, and the peak position moves towards higher energy a little for $M_{\text{inv}} = 2050$ MeV. In the case of the $\pi^+ \Sigma^-$ and $\pi^- \Sigma^+$ final state, while the basic features are shared with the $\pi^0 \Sigma^0$, the peak positions of the $\pi^+ \Sigma^-$ mass distribution are about 5 MeV less than that of the $\pi^0 \Sigma^0$ mass distribution, and the peak positions in the $\pi^- \Sigma^+$ mass distribution are about 5 MeV bigger than the values of the $\pi^0 \Sigma^0$ mass distribution with a similar width and strength. Among these processes, the $\pi^+ \Sigma^-$ gives the largest strength. This is roughly because the $t_{\Sigma^- \pi^+, \Sigma \pi}$ term is twice larger than $t_{\Sigma^0 \pi^0, \Sigma \pi}$ in Eq. (II.30).

In Fig. 7, we show the results of $\frac{d^2 \sigma_{pK^+ \pi\Sigma}}{dM_{\text{inv}} dm_{\text{inv}}}$ for the $pp \rightarrow pK^+ \pi\Sigma$ scattering as a functions of $m_{\text{inv}}(\pi^0 \Sigma^0)$, $m_{\text{inv}}(\pi^+ \Sigma^-)$ and $m_{\text{inv}}(\pi^- \Sigma^+)$, respectively. The total energy of the system \sqrt{s} is fixed at 3179 MeV which can be accessed experimentally [64–66]. The dependence on m_{inv} is similar to that in $d\sigma_{K^0 \pi\Sigma} / dm_{\text{inv}}$. In the case of the $\pi^0 \Sigma^0$ the peak is located at 1400 MeV by fixing $M_{\text{inv}} = 2140$ MeV. For $M_{\text{inv}} = 2200$ and 2230 MeV, the peak positions move towards 1380 MeV and also the widths are broader than that of the 1400 MeV case. Decreasing the value of M_{inv} to 2100 MeV, we obtain

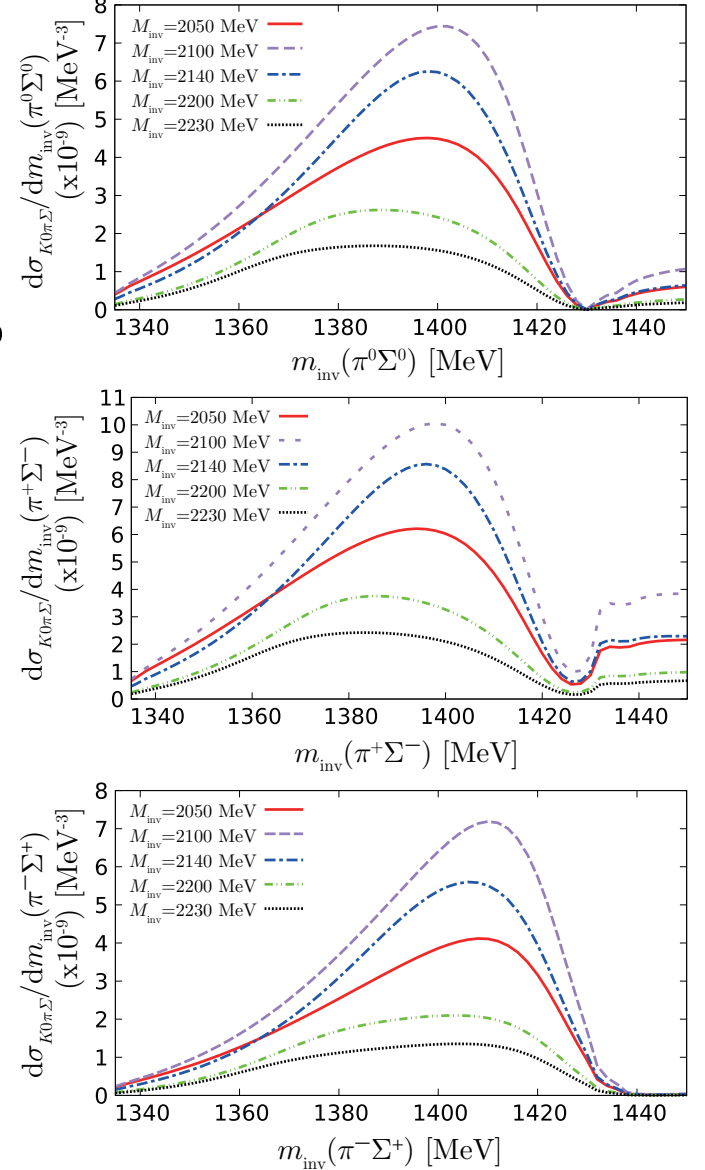


FIG. 6: The $\frac{d\sigma}{dm_{\text{inv}}}$ mass distribution as a function of $m_{\text{inv}}(\pi^0 \Sigma^0)$, $m_{\text{inv}}(\pi^+ \Sigma^-)$ and $m_{\text{inv}}(\pi^- \Sigma^+)$ for the $\pi^- p \rightarrow K^0 \pi\Sigma$ scattering with several fixed values of M_{inv} .

the peak position around 1405 MeV. The shape of results are similar for the $\pi^+ \Sigma^-$ and $\pi^- \Sigma^+$ mass distributions, but the peak positions are 10 MeV bigger for the case of $\pi^+ \Sigma^-$ and 5 MeV smaller for $\pi^- \Sigma^+$ mass distribution. In these processes, the $\pi^- \Sigma^+$ gives the largest strength because of the additional factor two for the $t_{\Sigma^+ \pi^-, \Sigma \pi}$ term in Eq. (II.48) compared with $t_{\Sigma^0 \pi^0, \Sigma \pi}$. We should note that the peak with this mechanism appears at lower $\pi\Sigma$ invariant mass than with the model

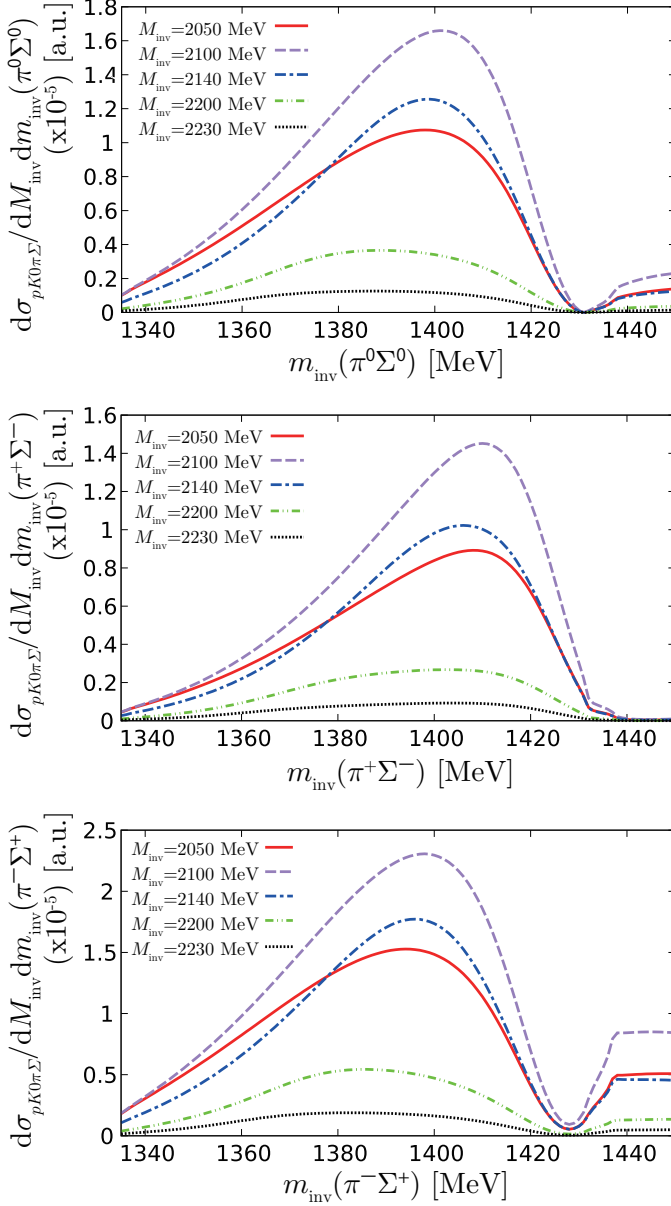


FIG. 7: The $\frac{d^2\sigma_{pK^+\pi\Sigma}}{dM_{\text{inv}}dm_{\text{inv}}}$ as a function of $m_{\text{inv}}(\pi^0\Sigma^0)$, $m_{\text{inv}}(\pi^+\Sigma^-)$ and $m_{\text{inv}}(\pi^-\Sigma^+)$ for the $pp \rightarrow pK^+\pi\Sigma$ scattering with several fixed values of M_{inv} and $\sqrt{s} = 3179$ MeV.

of [75], where the peak showed at 1420 MeV. This is due to the fact that with the TS the $\Lambda(1405)$ is formed by $\pi\Sigma$, rather than $\bar{K}N$, and this channel couples mostly to the lower mass state of the two $\Lambda(1405)$ states [10].

For the case of the $\pi^-p \rightarrow K^0\pi\Sigma$ reaction, we integrate $\frac{d\sigma_{K^0\pi\Sigma}}{dm_{\text{inv}}}$ over m_{inv} in the range of the $\Lambda(1405)$ peak, $m_{\text{inv}} \in (m_\pi + m_\Sigma, 1450)$ MeV, with m_π and m_Σ

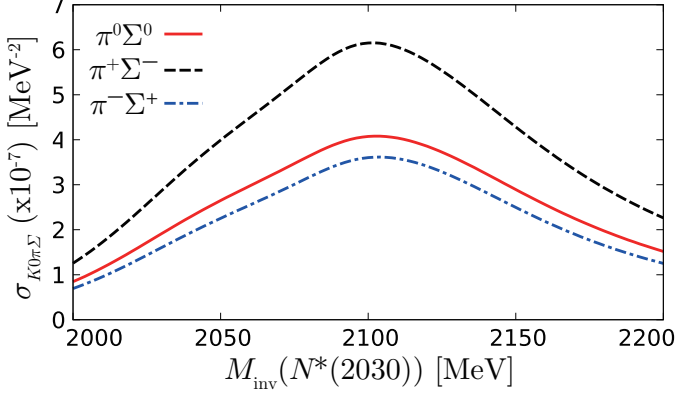


FIG. 8: The cross section of the $\pi^-p \rightarrow K^0\pi\Sigma$ process $\sigma_{K^0\pi\Sigma}$ as a function of M_{inv} for the $\pi^-p \rightarrow K^0\pi\Sigma$ scattering. The red solid line corresponds to the $\pi^0\Sigma^0$, the black dash line the $\pi^+\Sigma^-$ and the blue dash-dot line $\pi^-\Sigma^+$.

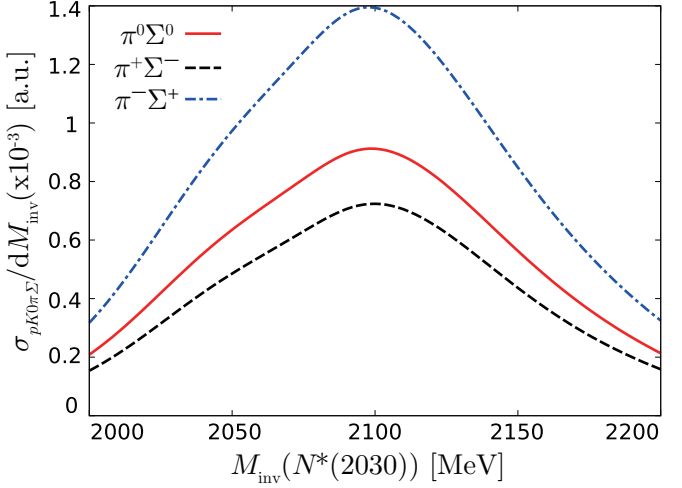


FIG. 9: The $\frac{d\sigma_{pK^+\pi\Sigma}}{dM_{\text{inv}}}$ as a function of M_{inv} for the $pp \rightarrow pK^+\pi\Sigma$ scattering with fixed value of $\sqrt{s} = 3179$ MeV. The red solid line corresponds to the $\pi^0\Sigma^0$, the black dash line the $\pi^+\Sigma^-$ and the blue dash-dot line $\pi^-\Sigma^+$.

the isospin-averaged mass of π and Σ , and we obtain the cross section of $\pi^-p \rightarrow K^0\pi\Sigma$, $\sigma_{K^0\pi\Sigma}$, as a function of M_{inv} . The results are represented in Fig. 8. There are peaks around 2100 MeV for all cases, though the expected value of triangular singularity is 2140 MeV. This is because the N^* resonance in the $K^*\Sigma$ production has a peak around 2030 MeV (the term $1/|M_{\text{inv}} - M_{N^*} + i\frac{\Gamma_{N^*}}{2}|^2$ in Eq. (II.48)).

For the case of the $pp \rightarrow pK^+\pi\Sigma$ reaction, integrating

now the $\frac{d^2\sigma_{pK^+\pi\Sigma}}{dM_{\text{inv}}dm_{\text{inv}}}$ over the m_{inv} we obtain $\frac{d\sigma_{pK^+\pi\Sigma}}{dM_{\text{inv}}}$ which are shown in Fig. 9 as a function of M_{inv} for $\pi^0\Sigma^0$, $\pi^+\Sigma^-$ and $\pi^-\Sigma^+$. Similarly we get peaks around 2100 MeV for the three cases.

In the π^-p and pp reactions, the strength is largest for the $\pi^+\Sigma^-$ and $\pi^-\Sigma^+$ final state, respectively, reflecting the strength before the integration shown in Figs. 6 and 7.

IV. SUMMARY

We have carried out a study of contributions of a triangle diagram to the the $\pi^-p \rightarrow K^0\pi\Sigma$ and $pp \rightarrow pK^+\pi\Sigma$ processes. In both reactions, the triangle diagram is formed by the N^* decaying first to K^* and Σ , the K^* decays into πK , and then the Σ and the π merge to give $\Lambda(1405)$, which finally decays into $\pi\Sigma$. In this process, the $K^*\pi\Sigma$ loop generates a triangle singularity around 2140 MeV in the invariant mass of $K\Lambda(1405)$ from the formula of Eq. (18) of Ref. [53]. We evaluate the real, imaginary part and absolute value of the amplitude t_T and find a peak around 2140 MeV.

We calculate the $\frac{d\sigma_{K^0\pi\Sigma}}{dM_{\text{inv}}}$ with some values of M_{inv}

in the $\pi^-p \rightarrow K^0\pi\Sigma$ reaction and $\frac{d^2\sigma_{pK^+\pi\Sigma}}{dM_{\text{inv}}dm_{\text{inv}}}$ with some values of M_{inv} and fixed $\sqrt{s} = 3179$ MeV as a function of $m_{\text{inv}}(\pi^0\Sigma^0)$, $m_{\text{inv}}(\pi^+\Sigma^-)$ and $m_{\text{inv}}(\pi^-\Sigma^+)$. In these distributions, we see peaks around 1400 MeV, representing clearly the $\Lambda(1405)$. Integrating over the

m_{inv} we obtain $\sigma_{K^0\pi\Sigma}$ and $\frac{d\sigma_{pK^+\pi\Sigma}}{dM_{\text{inv}}}$ and these distributions show a clear peak for $M_{\text{inv}}(N^*(2030))$ around 2100 MeV. The peak of the singularity shows up around 2140 MeV. This peak position of the triangular singularity is lowered by the initial N^* resonance peak around 2030 MeV in the $K^*\Sigma$ production.

Thus, our results constitute an interesting prediction of the triangle singularity effect in the cross sections of these decays. The work done here could explain why in the experiments of Refs. [65, 66] the invariant mass distribution of $\pi\Sigma$ for the $\Lambda(1405)$ are found at lower invariant masses than in other reactions. It would also be interesting to see if the predictions done here concerning the triangle singularity are fulfilled by the experimental data, an issue that has not been investigated so far. This work also can serve as a warning to future experiments that measure these interactions, that they should be careful when associating peaks in this energy region to resonances.

Acknowledgements

R.P. Pavao wishes to thank the Generalitat Valenciana in the program Santiago Grisolía. This work is partly supported by the Spanish Ministerio de Economía y Competitividad and European FEDER funds under the contract number FIS2014-57026-REDT, FIS2014-51948-C2-1-P, and FIS2014-51948-C2-2-P, and the Generalitat Valenciana in the program Prometeo II-2014/068.

- [1] N. Isgur and G. Karl, Phys. Rev. D **18** (1978) 4187.
- [2] R. H. Dalitz and S. F. Tuan, Phys. Rev. Lett. **2** (1959) 425.
- [3] R. H. Dalitz and S. F. Tuan, Annals Phys. **10** (1960) 307.
- [4] R. H. Dalitz, T. C. Wong and G. Rajasekaran, Phys. Rev. **153** (1967) 1617.
- [5] N. Kaiser, P. B. Siegel and W. Weise, Nucl. Phys. A **594**, 325 (1995) [nucl-th/9505043].
- [6] E. Oset and A. Ramos, Nucl. Phys. A **635**, 99 (1998) [nucl-th/9711022].
- [7] J. A. Oller and U. G. Meißner, Phys. Lett. B **500**, 263 (2001) [hep-ph/0011146].
- [8] M. F. M. Lutz and E. E. Kolomeitsev, Nucl. Phys. A **700**, 193 (2002) [nucl-th/0105042].
- [9] C. García-Recio, J. Nieves, E. Ruiz Arriola and M. J. Vicente Vacas, Phys. Rev. D **67**, 076009 (2003) [hep-ph/0210311].
- [10] D. Jido, J. A. Oller, E. Oset, A. Ramos and U. G. Meißner, Nucl. Phys. A **725** (2003) 181 [nucl-th/0303062].
- [11] B. Borasoy, R. Nissler and W. Weise, Eur. Phys. J. A **25**, 79 (2005) [hep-ph/0505239].
- [12] Y. Ikeda, T. Hyodo, D. Jido, H. Kamano, T. Sato and K. Yazaki, Prog. Theor. Phys. **125** (2011) 1205 [arXiv:1101.5190 [nucl-th]].
- [13] Y. Ikeda, T. Hyodo and W. Weise, Nucl. Phys. A **881**, 98 (2012) [arXiv:1201.6549 [nucl-th]].
- [14] Z. H. Guo and J. A. Oller, Phys. Rev. C **87**, no. 3, 035202 (2013) [arXiv:1210.3485 [hep-ph]].
- [15] A. Feijoo, V. K. Magas and A. Ramos, Phys. Rev. C **92**, no. 1, 015206 (2015) [arXiv:1502.07956 [nucl-th]].
- [16] M. Mai and U. G. Meißner, Eur. Phys. J. A **51**, no. 3, 30 (2015) [arXiv:1411.7884 [hep-ph]].
- [17] J. M. M. Hall, W. Kamleh, D. B. Leinweber, B. J. Menadue, B. J. Owen, A. W. Thomas and R. D. Young, Phys. Rev. Lett. **114** (2015) no.13, 132002 [arXiv:1411.3402 [hep-lat]].
- [18] R. Molina and M. Döring, Phys. Rev. D **94** (2016) no.5, 056010 Addendum: [Phys. Rev. D **94** (2016) no.7, 079901] [arXiv:1512.05831 [hep-lat]].
- [19] T. Sekihara, T. Hyodo and D. Jido, PTEP **2015** (2015) 063D04 [arXiv:1411.2308 [hep-ph]].

[20] Z. H. Guo and J. A. Oller, Phys. Rev. D **93** (2016) no.9, 096001 [arXiv:1508.06400 [hep-ph]].

[21] Y. Kamiya and T. Hyodo, Phys. Rev. C **93** (2016) no.3, 035203 [arXiv:1509.00146 [hep-ph]].

[22] T. Sekihara, T. Hyodo and D. Jido, Phys. Lett. B **669** (2008) 133 [arXiv:0803.4068 [nucl-th]].

[23] K. Miyahara and T. Hyodo, Phys. Rev. C **93** (2016) no.1, 015201 [arXiv:1506.05724 [nucl-th]].

[24] J. C. Nacher, E. Oset, H. Toki and A. Ramos, Phys. Lett. B **455** (1999) 55 [nucl-th/9812055].

[25] J. C. Nacher, E. Oset, H. Toki and A. Ramos, Phys. Lett. B **461** (1999) 299 [nucl-th/9902071].

[26] B. Borasoy, P. C. Bruns, U. G. Meißner and R. Nissler, Eur. Phys. J. A **34** (2007) 161 [arXiv:0709.3181 [nucl-th]].

[27] L. Roca and E. Oset, Phys. Rev. C **87** (2013) no.5, 055201 [arXiv:1301.5741 [nucl-th]].

[28] S. X. Nakamura and D. Jido, PTEP **2014** (2014) 023D01 [arXiv:1310.5768 [nucl-th]].

[29] E. Wang, J. J. Xie, W. H. Liang, F. K. Guo and E. Oset, Phys. Rev. C **95** (2017) no.1, 015205 [arXiv:1610.07117 [hep-ph]].

[30] T. Hyodo, A. Hosaka, E. Oset, A. Ramos and M. J. Vicente Vacas, Phys. Rev. C **68** (2003) 065203 [nucl-th/0307005].

[31] V. K. Magas, E. Oset and A. Ramos, Phys. Rev. Lett. **95** (2005) 052301 [hep-ph/0503043].

[32] D. Jido, E. Oset and T. Sekihara, Eur. Phys. J. A **42** (2009) 257 [arXiv:0904.3410 [nucl-th]].

[33] K. Miyagawa and J. Haidenbauer, Phys. Rev. C **85** (2012) 065201 [arXiv:1202.4272 [nucl-th]].

[34] D. Jido, E. Oset and T. Sekihara, Eur. Phys. J. A **49** (2013) 95 [arXiv:1207.5350 [nucl-th]].

[35] S. Ohnishi, Y. Ikeda, T. Hyodo and W. Weise, Phys. Rev. C **93** (2016) no.2, 025207 [arXiv:1512.00123 [nucl-th]].

[36] L. S. Geng and E. Oset, Eur. Phys. J. A **34** (2007) 405 [arXiv:0707.3343 [hep-ph]].

[37] J. Siebenstar and L. Fabbietti, Phys. Rev. C **88** (2013) 055201 [arXiv:1306.5183 [nucl-ex]].

[38] K. Miyahara, T. Hyodo and E. Oset, Phys. Rev. C **92** (2015) no.5, 055204 [arXiv:1508.04882 [nucl-th]].

[39] T. Hyodo and D. Jido, Prog. Part. Nucl. Phys. **67** (2012) 55 [arXiv:1104.4474 [nucl-th]].

[40] Y. Kamiya, K. Miyahara, S. Ohnishi, Y. Ikeda, T. Hyodo, E. Oset and W. Weise, Nucl. Phys. A **954** (2016) 41 [arXiv:1602.08852 [hep-ph]].

[41] U.-G. Meißner, T. Hyodo, Pole Structure of the (1405) Region, C. Patrignani et al. (Particle Data Group), Chin. Phys. C,40, 100001 (2016)

[42] L. D. Landau, Nucl. Phys. **13** (1959) 181.

[43] S. Coleman and R. E. Norton, Nuovo Cim. **38** (1965) 438.

[44] J. J. Wu, X. H. Liu, Q. Zhao and B. S. Zou, Phys. Rev. Lett. **108** (2012) 081803 [arXiv:1108.3772 [hep-ph]].

[45] F. Aceti, W. H. Liang, E. Oset, J. J. Wu and B. S. Zou, Phys. Rev. D **86** (2012) 114007 [arXiv:1209.6507 [hep-ph]].

[46] X. G. Wu, J. J. Wu, Q. Zhao and B. S. Zou, Phys. Rev. D **87** (2013) no.1, 014023 [arXiv:1211.2148 [hep-ph]].

[47] Q. Wang, C. Hanhart and Q. Zhao, Phys. Rev. Lett. **111** (2013) no.13, 132003 [arXiv:1303.6355 [hep-ph]].

[48] X. H. Liu and G. Li, Phys. Rev. D **88** (2013) 014013 [arXiv:1306.1384 [hep-ph]].

[49] X. H. Liu, M. Oka and Q. Zhao, Phys. Lett. B **753** (2016) 297 [arXiv:1507.01674 [hep-ph]].

[50] F. K. Guo, U. G. Meißner, W. Wang and Z. Yang, Phys. Rev. D **92** (2015) no.7, 071502 [arXiv:1507.04950 [hep-ph]].

[51] X. H. Liu, Q. Wang and Q. Zhao, Phys. Lett. B **757** (2016) 231 [arXiv:1507.05359 [hep-ph]].

[52] F. K. Guo, U. G. Meißner, J. Nieves and Z. Yang, Eur. Phys. J. A **52** (2016) no.10, 318 [arXiv:1605.05113 [hep-ph]].

[53] M. Bayar, F. Aceti, F. K. Guo and E. Oset, Phys. Rev. D **94** (2016) no.7, 074039 [arXiv:1609.04133 [hep-ph]].

[54] R. Aaij *et al.* [LHCb Collaboration], Phys. Rev. Lett. **115** (2015) 072001 [arXiv:1507.03414 [hep-ex]].

[55] X. H. Liu and U. G. Meißner, arXiv:1703.09043 [hep-ph].

[56] S. Sakai, E. Oset and A. Ramos, arXiv:1705.03694 [hep-ph].

[57] R. Pavao, S. Sakai and E. Oset, Eur. Phys. J. C **77** (2017) no.9, 599 [arXiv:1706.08723 [hep-ph]].

[58] D. Gamermann, E. Oset, D. Strottman and M. J. Vicente Vacas, Phys. Rev. D **76** (2007) 074016 [hep-ph/0612179].

[59] D. Gamermann and E. Oset, Eur. Phys. J. A **33** (2007) 119 [arXiv:0704.2314 [hep-ph]].

[60] E. Oset and A. Ramos, Eur. Phys. J. A **44** (2010) 445 [arXiv:0905.0973 [hep-ph]].

[61] A. Ramos and E. Oset, Phys. Lett. B **727** (2013) 287 [arXiv:1304.7975 [nucl-th]].

[62] A. Engler, H. E. Fisk, R. W. Kraemer, C. M. Meltzer and J. B. Westgard, Phys. Rev. Lett. **15** (1965) 224.

[63] D. W. Thomas, A. Engler, H. E. Fisk and R. W. Kraemer, Nucl. Phys. B **56** (1973) 15.

[64] I. Zychor *et al.*, Phys. Lett. B **660** (2008) 167 [arXiv:0705.1039 [nucl-ex]].

[65] G. Agakishiev *et al.* [HADES Collaboration], Phys. Rev. C **87** (2013) 025201 [arXiv:1208.0205 [nucl-ex]].

[66] J. Adamczewski-Musch *et al.* [HADES Collaboration], Phys. Rev. C **95** (2017) no.1, 015207 [arXiv:1611.01040 [nucl-ex]].

[67] M. Bando, T. Kugo and K. Yamawaki, Phys. Rept. **164** (1988) 217.

[68] U. G. Meißner, Phys. Rept. **161** (1988) 213.

[69] H. Nagahiro, L. Roca, A. Hosaka and E. Oset, Phys. Rev. D **79** (2009) 014015 [arXiv:0809.0943 [hep-ph]].

[70] M. Bando, T. Kugo, S. Uehara, K. Yamawaki and T. Yanagida, Phys. Rev. Lett. **54** (1985) 1215.

[71] F. Aceti, J. M. Dias and E. Oset, Eur. Phys. J. A **51** (2015) no.4, 48 [arXiv:1501.06505 [hep-ph]].

[72] V. R. Debastiani, F. Aceti, W. H. Liang and E. Oset, Phys. Rev. D **95** (2017) no.3, 034015 [arXiv:1611.05383 [hep-ph]].

[73] F. Mandl and G. Shae, *Quantum Field Theory*. John Wiley and sons, 1984

[74] R. P. Pavao, W. H. Liang, J. Nieves and E. Oset, Eur. Phys. J. C **77** (2017) no.4, 265 [arXiv:1701.06914 [hep-ph]].

[75] L. S. Geng and E. Oset, Eur. Phys. J. A **34** (2007) 405

[arXiv:0707.3343 [hep-ph]].